Enhancement strategies for the microbial protein production of nitrogen-fixing hydrogen-oxidizing bacterial community

Abstract

The feasibility and superiority of utilizing nitrogen-fixing hydrogen-oxidizing bacteria (NF-HOB) for microbial protein (MP) production have been proposed. This study simulated air as the source of nitrogen and oxygen and enhanced production efficiency by employing key strategies, including continuous gas supply, selecting a higher hydrogen-to-oxygen ratio, designing initial community structures and domestication, and exploring appropriate hydraulic retention times (HRT) in continuous culture. The results demonstrated that sequencing batch culture achieved an MP titer of 0.98 g/L, with N_2 fixation efficiency surpassing natural nodules by two orders of magnitude at 1.6 mg N_2 per g dry biomass per hour. Under an HRT of 48 hours, MP volumetric productivity reached 2.297 mg/(L·h), accompanied by a maximum biomass yield of 0.11 g CDW/g COD-H_2. The high abundance of nitrogenase may provide crucial functional support, enabling the NF-HOB community to exhibit potential beyond previous understanding.

Keywords: Hydrogen-oxidizing bacteria; Nitrogen fixation; Microbial protein; Hydrogen-to-oxygen ratio; Hydraulic retention time

1. Introduction

Hydrogen-oxidizing bacteria (HOB) have recently attracted significant attention for their ability to utilize renewable hydrogen energy for carbon dioxide fixation and their potential in the synthesizing high-quality microbial protein (MP) (Matassa et al., 2015; Woern and Grossmann, 2023). However, a majority of HOB employed for MP production still necessitate energy-intensive inputs (Hu et al., 2020; Sherbo et al., 2022), particularly ammonium salts derived from the Haber-Bosch process as an optimal nitrogen source. This practice leads to carbon dioxide emissions, contradicting the inherent advantages of autotrophic bacteria as nutrient producers.

Therefore, the advantages of nitrogen-fixing hydrogen-oxidizing bacteria (NF-HOB), also known as "H-C-N microorganisms" (Sherbo et al., 2022), have been further proposed. This group includes members from the following genera: *Azospirillum* (*Azospirillum lipoferum*), *Ancylobacter* (*Ancylobacter aquaticus*, *Ancylobacter vacuolatus*), *Xanthobacter* (*Xanthobacter autotrophicus*, *Xanthobacter flavus*, *Xanthobacter variabilis*), *Bradyrhizobium* (*Bradyrhizobium japonicum*), *Azohydromonas* (*Azohydromonas lata*), and *Derxia* (*Derxia gummosa*) (Hu et al., 2022; Lu et al., 2020; Malik and Schlegel, 1981; Scott et al., 2021). Cultivation experiments are essential for identifying NF-HOB, as they allow for determining their ability to simultaneously fix CO_2 and N_2 under hydrogen autotrophic conditions for growth. Utilizing NF-HOB for MP production represents a highly sustainable approach that effectively harnesses the abundant atmospheric resources of N_2 and O_2, integrating hydrogen production technology with MP synthesis regardless of climate or geographical constraints. Notably, when solar energy is used for hydrogen production

technology, the solar-to-biomass energy conversion efficiency of NF-HOB was more than double that observed in symbiotic N_2-fixing soybeans (Hu et al., 2020).

Currently, cultivating NF-HOB is still in the experimental phase within small-scale systems. Hu et al. successfully achieved enrichment of NF-HOB community under headspace gas supply conditions (2% O_2, 10% H_2, 10% CO_2, 78% N_2) in serum bottles, resulting in a protein-rich biomass with an amino acid profile comparable to that of MP derived from ammonium-based HOB. However, biomass growth under this system was significantly constrained, with the titer of nitrogen content in biomass being less than 12 mg/L (Hu et al., 2020). Recently, a comparative experiment was conducted in a continuous gas supply system to evaluate nitrogen source supply conditions. The results showed a slightly higher N_2 fixation amount in the simple device compared to previous studies, confirming the potential of continuous feed gas for enriching NF-HOB. Importantly, no significant difference was observed in the absolute abundance of hydrogenase or Rubisco between the NF-HOB community and the control community supplied with ammonia nitrogen, suggesting that the synthesis of essential functional enzymes was not limited. Furthermore, it is noteworthy that air can potentially substitute separately supplied N_2 and O_2 based on a feed gas composition of $H_2/O_2/CO_2/N_2$ = 6/1/1.56/4.28 (v/v/v/v) (Wang et al., 2024).

It should be emphasized that, considering the future potential of large-scale utilization of NF-HOB for MP production, developing a functionally stable microbial community offers greater advantages in mitigating external pollution compared to pure strains (Matassa et al., 2015). Optimizing the hydrogen-oxygen ratio ($R_{H/O}$) in the feed gas and exploring cultivation in a continuous reactor are promising strategies for

enhancing MP production based on NF-HOB community, considering the influence of feed gas component proportions on functional enzyme activity and the promoting effect of continuous culture mode for the ammonium-based HOB community (Matassa et al., 2016).

This study employed a more efficient gas-liquid mass transfer fermentation system and incorporated a N_2-O_2 mixed gas with a ratio of 4:1 to simulate the feasibility of air inclusion in the feed gas. Furthermore, deliberate design and acclimation were applied to the initial bacterial community structure to enhance its N_2 fixation activity. Subsequently, the performance of NF-HOB community in producing MP under slightly lower or higher $R_{H/O}$ (3.5 and 7, respectively) compared to previous studies ($R_{H/O}$ = 5 or 6) was investigated in sequencing batch culture, with ammonium provision as the comparative condition. Additionally, the effective hydraulic retention time (HRT) was investigated in continuous cultivation while simultaneously assessing volumetric productivity and biomass yield. An analysis of the impact of these enhancement strategies on the microbial community structure was conducted, accompanied by a description of functional abundance characteristics to provide mechanistic support. The research findings revealed significant potential for synthesizing MP based on NF-HOB, surpassing previous understanding.

2. Material and methods

2.1 Design and domestication of initial microbial community

The NF-HOB community obtained from the previous study was combined with the laboratory-preserved NF-HOB strains (*Xanthobacter flavus* strain CIB1 [GenBank:

OP108817.1] and unclassified Xanthobacteraceae bacterium strain CIB2) and subsequently inoculated into a device previously used for enriching NF-HOB (Wang et al., 2024). The flow rates of each component in the continuously supplied feed gas were: H_2 81 mL/min, O_2 13.5 mL/min, CO_2 21 mL/min, N_2 57.75 mL/min ($R_{H/O}$ = 6). The components of the base medium included: K_2HPO_4 1 g/L, KH_2PO_4 0.5 g/L, $NaHCO_3$ 2 g/L, $MgCl_2{\cdot}6H_2O$ 0.12 g/L, $CaCl_2$ 0.0258 g/L, $NaVO_3{\cdot}H_2O$ 50 mg/L, $Na_2MoO_4{\cdot}2H_2O$ 25 mg/L, $FeSO_4{\cdot}7H_2O$ 50mg /L, vitamin solution and trace element solution both added at 1mL/L. Cultivation was carried out at a constant temperature of 30 □ for one month.

The cultivation process demonstrated a significant increase in turbidity, indicating the community's potential for growth under hydrogen autotrophy and nitrogen fixation conditions after domestication, making it suitable for subsequent quantitative experiments.

2.2 Sequencing batch culture

The gas fermentation system constituted the primary component of the reactors (see supplementary material). Each glass fermentation tank was equipped with three agitators, each featuring four-blade impellers, as well as a thermometer, a pH meter, and an aeration device. The stirring speed and temperature were controlled by the fermentation system at 500 rpm and 30 □, respectively. The gas cylinder continuously supplied H_2, N_2-O_2 mixed gas (4:1, simulated air), and CO_2, which were thoroughly mixed after passing through pipelines, flow-stabilizing valves, and rotameters in sequential order as previously described (Wang et al., 2024). The mixture was then introduced into the fermentation tank. The flow rate of each gas component was

adjusted by manipulating the valve and rotameter to precisely regulate $R_{H/O}$. Exhaust gases were collected using gas collection bags that demonstrated excellent airtightness.

In order to better evaluate the growth trend, two fermentation tanks were utilized with the base medium and base medium supplemented with 2 g/L NH_4Cl (2 L, pH adjusted to 7.5 using 1 mol/L hydrochloric acid prior to inoculation). Consequently, ammonium assimilation conditions were employed as the control for nitrogen fixation conditions. Consistent initial inoculation and gas intake were maintained in both tanks.

Under low $R_{H/O}$ (3.5) conditions, the total flow rates of H_2, "air", and CO_2 prior to distribution into the two fermentation tanks were 42 mL/min, 60 mL/min, and 20 mL/min, respectively. In contrast, under high $R_{H/O}$ (7) conditions, the flow rate of "air" was adjusted to 30 mL/min.

During the batch cultivation period, daily samples were collected from the fermentation tank to quantify total chemical oxygen demand (COD_t) and cell dry weight (CDW) for biomass titer characterization, while monitoring pH. The collected samples were filtered using a membrane filter (0.22 μm Nylon66, JINTENG, China) and then analyzed for soluble chemical oxygen demand (COD_s), nitrate nitrogen, nitrite nitrogen, and ammonia nitrogen. Biomass measurement at the end of cultivation necessitated transferring the bacteria that had been suspended and adhered to the tank wall due to agitation into the liquid phase and thoroughly homogenizing before sampling.

2.3 Continuous culture

For the continuous reactor, the liquid flow rate was controlled through the control panel (see supplementary material), allowing automated operation of the peristaltic

pumps and ensuring equal amounts of fresh base medium and culture solution in and out of the system. The liquid phase volume was stabilized at 2 L; thus, the required liquid flow rate can be determined based on HRT. The other cultivation conditions were consistent with those used in batch culture.

The community that exhibited stable proliferation in the sequencing batch culture was utilized as the inoculum source. Samples were collected from both the inner liquid phase and the collector for liquid discharge in order to measure COD_t (inner) and daily average COD_t (outlet), respectively.

2.4 Quantification of H_2 utilization

Referring to previous NF-HOB research, the quantification of H_2 consumption corresponding to biomass growth was conducted through cultivation experiments in anaerobic flasks to determine the biomass yield (Hu et al., 2020; Wang et al., 2024). The proportion of each component in the headspace gas followed that of the continuous gas supply system and was cultured in a constant temperature shaker (30 □, 180 rpm). The headspace gas was updated every two days with the total effective cultivation time of 6 days. For NF-HOB communities obtained from sequencing batch culture and continuous culture, measurements were taken for CDW, COD_t, and pH at both the beginning and end of the culture period. This experiment was performed in triplicate.

2.5 Analysis and characterization of MP

The carbon and nitrogen content in the biomass was determined using an elemental analyzer (vario EL cube, ELEMENTAR, Germany). The obtained nitrogen

content was then multiplied by a conversion coefficient of 6.25 to determine the MP content (Matassa et al., 2016). The dietary amino acid composition of the biomass was determined by Baihui Biotech (Chengdu, China).

2.6 Microbial community analysis

The bacterial solutions to be analyzed were each sampled with a minimum volume of 50 mL, followed by centrifugation for supernatant removal and subsequent storage at -80 °C. DNA extraction of culture samples and Illumina NovaSeq sequencing were performed by Novogene (Beijing, China). MetaStat analysis was used to identify species with significantly different abundances between groups. Functional annotation of PICRUST2 was employed to reflect the abundance of important functional enzymes or their coding genes.

2.7 Analytical methods and calculations

The concentrations of COD_t and COD_s were determined using the COD detection kit (Titric, China). The pH value was determined using a pH meter (Seven2Go, METTLER TOLEDO, Switzerland). The concentrations of NH_4^+-N, NO_3^- -N, and NO_2^- -N were determined using Nessler reagent spectrophotometry, ultraviolet spectrophotometry, and N-(1-naphthyl)-ethylenediamine photometry techniques, respectively. CDW determination was accomplished by desiccating and quantifying a fixed volume sample, as previously described (Wang et al., 2024).

In the liquid phase, the total nitrogen (TN) is calculated as: TN = Total nitrogen content of biomass ($TN_{biomass}$) + NH_4^+-N (AN) + NO_3^--N + NO_2^--N; soluble total nitrogen (TN_s) = AN + NO_3^--N + NO_2^--N, $TN_{biomass}$ (mg/L) = N content (%) ×

CDW (mg/L).

NH_4^+ -N conversion efficiency (%) = (initial AN concentration – final AN concentration) / initial AN concentration; NH_4^+-N utilization efficiency (%) = increased $TN_{biomass}$ / (initial AN concentration – final AN concentration). Biomass yield (g CDW/g COD-H_2) = increased CDW (mg) / [8 (g COD/g H_2) × reduced H_2 (mg)].

3. Results and discussion

3.1 A high hydrogen-oxygen ratio facilitated microbial protein production with high titers

O_2 exerts inhibitory effects on both hydrogenase (Greening et al., 2023; Zacarias et al., 2019) and nitrogenase (Allen et al., 2019), while also competing to inhibit the CO_2 reduction activity of Rubisco (Poudel et al., 2020). However, low concentrations of O_2 can result in insufficient electron acceptors. Therefore, optimizing the $R_{H/O}$ of feed gas is a primary strategy to consider.

The autotrophic growth of *Xanthobacter* in a gas mixture with an $H_2/O_2/CO_2$ ratio of 7/2/1 was initially documented (Wiegel et al., 1978). Additionally, the H/O ratio observed in the biomass composition of various HOB strains ranged from 2.71 to 3.77 (Ishizaki and Tanaka, 1990; Yu and Lu., 2019; Zhang et al., 2020b). However, results from sequencing batch culture experiments revealed that an $R_{H/O}$ of 3.5 solely facilitated ammonium assimilation without supporting biomass growth during N_2 fixation.

Under N_2 fixation conditions, COD_t gradually increased, reaching only 158 mg/L over 10 days, while pH fluctuated around 7.6. In the presence of ammonia nitrogen,

both COD_t and CDW rapidly increased, reaching 4552 mg/L and 2360 mg/L, respectively, on the 10th day. Notably, efficient CO_2 absorption during this period caused the culture medium's pH to decline from 7.88 to 6.12 (Fig. 1A). The observed difference surpassed previous studies' outcomes, likely due to the lower $R_{H/O}$.

The nitrogen transformation process aligned well with expectations, evidenced by the low concentration of TN_s (mainly NH_4^+-N) in the medium under N_2 fixation conditions (Fig. 1B) and a biomass titer of 305.56 mg/L (after three weeks of cultivation) with a nitrogen content of 6.41% (Fig. 1C). Consequently, most reduced N_2 was assimilated into the biomass, leading to a significant increase of 19.59 mg/L $TN_{biomass}$ ($\Delta TN_{biomass}$ – NF shown in Fig. 1D), surpassing previous research findings. The ammonium assimilation control exhibited remarkable efficiency in absorbing ammonium, achieving a conversion efficiency of 70.3% over ten days while maintaining very low levels of nitrate or nitrite nitrogen (Fig. 1B). Finally, the residual NH_4^+-N was measured at 116.5 mg/L, and CDW displayed a titer of 2410 mg/L (pH = 5.29) with a nitrogen content of 9.83% (Fig. 1C), resulting in an impressive ammonium utilization efficiency of 70.1% (Fig. 1D). Furthermore, biomass obtained under ammonium assimilation conditions exhibited a carbon and nitrogen composition more similar to that of *Cupriavidus necator* (previously named as *Alcaligenes europhus*) strain ATCC 17697T (Ishizaki and Tanaka, 1990), widely used as a reference for elucidating the stoichiometric relationship of HOB, rather than under N_2 fixation conditions (Fig. 1C).

Adjusting $R_{H/O}$ to 7 significantly enhanced the N_2-fixing capacity of the NF-HOB community, leading to increased biomass accumulation and MP synthesis. In the first

batch, following a lag period of approximately 9 days, the NF-HOB community exhibited rapid linear biomass growth, accompanied by a significant decrease in pH (Fig. 2A). By the 15th day, COD_t had increased impressively by 426% to 1299 mg/L. TN_s were remarkably low, primarily composed of ammonia nitrogen and nitrate nitrogen, as shown in Fig. 2D. The COD_t and CDW of the ammonium-assimilation HOB community continued to increase steadily; however, at a significantly slower rate compared to low $R_{H/O}$ conditions, reaching values of 2342 mg/L and 1760 mg/L on the 10th day, respectively. Consequently, there was also a reduction in pH decline (Fig. 2A). Surprisingly, the concentration of NH_4^+-N or TN_s increased by 82.5 mg/L in the initial 3 days (Fig. 2D), while biomass exhibited growth, suggesting this was due to N_2 fixation rather than bacterial lysis. This phenomenon is similar to observations in previous studies (Wang et al., 2024). The biomass accumulation of the NF-HOB community at the end of this batch was significantly enhanced, CDW reaching 1088.3 mg/L, thereby substantially reducing the disparity in biomass accumulation between NF-HOB and ammonium-assimilation HOB.

As for the second batch, over 14 days the NF-HOB community demonstrated remarkable increases in COD_t by 815% and CDW by 450% (Fig. 2B). During the latter half of the cultivation period, both NH_4^+-N and TN_s concentrations fluctuated and then increased, surpassing 10 mg/L on the 15th day (Fig. 2E). The growth rate of COD_t and CDW in the ammonium-assimilation HOB community closely approximated that observed in the first batch, while also showing fluctuations in NH_4^+-N concentration. Excitingly, after extending the culture for an additional 5 days, NF-HOB achieved a CDW titer of 1713 mg/L upon collection of adherent cells and bacterial fluid, closely

approaching the final titer of ammonium-assimilation HOB at 1725 mg/L – it is not uncommon for biomass to decrease with prolonged cultivation.

The biomass growth trend of the NF-HOB community in the third cultivation batch was similar to that observed in the second batch, demonstrating even greater increments in COD_t and CDW (Fig. 2C). The final concentration of COD_t was 3312 mg/L, with 2880 mg/L from $COD_{biomass}$ (the proportion of $COD_{biomass}$, always the main component, tended to be highest during the middle stage of cultivation, see supplementary material), resulting in a CDW titer of 2182 mg/L.

Elemental analysis revealed that the nitrogen content of NF-HOB biomass was slightly lower than that of ammonium-assimilation HOB, resulting in a higher C/N ratio. MP content significantly increased compared to results obtained under low $R_{H/O}$, ranging from 45.06% to 53.88% (Fig. 3A). By quantifying the nitrogen content in each component, it can be inferred that the NF-HOB community fixed more than 278 mg of N_2 in both of the last two batches (Fig. 3B), demonstrating substrate-based N_2 fixation efficiencies of 1.6 and 1.2 mg N_2 per g dry biomass per hour, respectively. This level exceeds that of natural nodules by two orders of magnitude (Lu et al., 2020). Fig. 3B also illustrates variations in TN_s and changes in $TN_{biomass}$ for ammonium-assimilation HOB communities, further substantiating the occurrence of N_2 fixation under conditions characterized by high $R_{H/O}$, which induced fluctuations in TN_s levels (Fig. 2D and 2E).

The amino acid composition of NF-HOB community biomass was compared to that of the NF-HOB community enriched by Hu et al. and soybean meal as reported in the literature (Hu et al., 2020; Karr-Lilienthal et al., 2005). Although the proportion of

essential and non-essential amino acids in the high-titer biomass in this study was slightly lower, its composition closely resembled that of soybean meal, exhibiting higher levels of valine, glycine, and alanine (Fig. 3C).

3.2 Appropriate setting of hydraulic retention time enables the feasibility of continuous cultivation

The specific growth rate of NF-HOB is evidently lower than that of ordinary HOB, making the previously commonly employed 10-hour HRT (Matassa et al., 2016) inapplicable. When HRT was set to 24 hours, only species with a specific growth rate of at least 0.042 were retained in the continuous reactor. The initial inoculation of biomass resulted in an initial COD_t of 186 mg/L; however, dilution over the next 4 days led to a daily reduction of half of the biomass in the reaction system. The average daily effluent COD_t (outlet) closely approximated the mean COD_t (inner) observed in the adjacent two-day system. Following re-inoculation to achieve an initial COD_t of 242 mg/L, a similar pattern of dilution was noted (Fig. 4A). Despite a decrease in the dilution rate, maintaining the inoculated biomass titer challenging when HRT was set to 36 hours. Furthermore, extending HRT to 48 hours resulted in NF-HOB accumulation. Once reaching a high density, it became difficult to reduce the HRT back to 36 hours while maintaining this density for more than a week; thus, 36 hours or less proved inadequate for supporting a stable reaction system. When HRT was set to 48 hours, the initial inoculation biomass measured COD_t at 99 mg/L. After a 2-day adaptation period, the community gradually enriched and achieved COD_t levels above 300 mg/L, reaching 328.58 mg/L on the 15th day. COD_s also accumulated progressively and accounted for over 25% of COD_t in later stages. The pH remained

consistently stable within the range of 7.10 to 7.45 (Fig. 4B). Therefore, under suitable conditions, NF-HOB exhibited a specific growth rate greater than 0.021. After 16 days of continuous cultivation, COD_t reached 383.65 mg/L and CDW reached 218.58 mg. The biomass obtained exhibited a carbon content of 42.6% and a nitrogen content of 8.07%, corresponding to an MP content of 50.44%. By collecting the solution containing this biomass concentration every 48 hours as the product, the volumetric productivity for MP was achieved at a rate of 2.297 mg/(L·h), surpassing that attained in batch culture. Although this value is significantly lower than the previously reported MP productivity of the ammonium-assimilation HOB community (Matassa et al., 2016), its predominance relies on the stable biomass concentration. Given that the HRT of 48 hours has been demonstrated to support continuous cultivation of NF-HOB communities, opting for a larger inoculum size will inevitably augment stable biomass concentrations, promising high production efficiency in future large-scale practice.

The headspace gas supply experiment conducted in sealed bottles (introduced in section 2.4) demonstrated that, although biomass growth of NF-HOB from continuous culture was comparatively lower within the same time frame (see supplementary material), the efficiency of biomass synthesis based on H_2 was comparable to that obtained through sequencing batch culture (Fig. 4C). The range observed in this study (0.0369-0.1069 g CDW/g COD-H_2) is consistent with previous findings.

3.3 Microbial community analysis

The taxonomic composition of each enriched microbial community at the family and genus levels is illustrated in Fig. 5A and 5B, respectively. Among the community utilized as the inoculum source, the Xanthobacteraceae family constituted 76.7%,

while *Xanthobacter* accounted for merely 2.70% and *Pseudoxanthobacter* accounted for only 1.32%. Consequently, 95% of Xanthobacteraceae species belonged to unidentified genera, classified as "others".

Hydrogenophaga has consistently maintained dominance as the genus in ammonium-assimilation HOB communities. Under low $R_{H/O}$ conditions, Bacteroidota (53.6%) dominated the NF-HOB community, with *Flavobacterium* and *Leadbetterella* exhibiting relative abundances of 27.8% and 16.8%, respectively. *Flavobacterium* has been reported to possess capabilities for H_2 oxidation (Maimaiti et al., 2007) and N_2 fixation (Kämpfer et al., 2015; Sorkhoh et al., 2010); however, there is insufficient evidence to substantiate its CO_2 fixation ability. Currently, *Leadbetterella* remains poorly understood. Therefore, the role of CO_2 fixation may be assumed by *Bacillus* (Maheshwari et al., 2017), *Xanthobacter* (Lu et al., 2020), *Hydrogenophaga* (Ehsani et al., 2019; Zhang et al., 2022), etc.

Under high $R_{H/O}$ conditions, the phylum Proteobacteria regained dominance. In the first batch, *Hydrogenophaga* (39.3%), *Ferruginibacter* (18.1%), and *Xanthobacter* (13.1%) were enriched. Although similar COD_t growth and $\Delta TN_{biomass}$ were observed in the second and third batches, significant differences in community structure were noted. In the second batch, *Xanthobacter* emerged as the predominant genus, with a relative abundance of 43.3%. Simultaneously, *Pseudoxanthobacter*, also from the Xanthobacteraceae family, displayed a relative abundance of 4.9%. Moreover, *Stappia*, with a relative abundance of 6.8%, may occupy an ecological niche due to its potential for CO_2 fixation (Weber and King, 2007; Zhang et al., 2020a); however, the precise role of *Ferruginibacter* (6.1%) remains unclear. In the third batch, *Hydrogenophaga*

was re-enriched; additionally, *Leadbetterella*, *Terrimonas*, and *Xanthobacter* were identified as other genera with relative abundances exceeding 4%. Notably, the N_2 fixation capability of *Terrimonas* has recently been emphasized (Guo et al., 2024), providing insights into its functional significance within the NF-HOB community.

The structure of the NF-HOB community obtained under continuous cultivation remained relatively complex, with genera exhibiting relative abundances exceeding 4%, including *Azonexus* (23.0%), *Methanobrevibacter* (12.7%, specifically *Methanobrevibacter arboriphilus*), *Stappia* (11.5%), *Hydrogenophaga* (4.9%), and *Bdellovibrio* (4.6%, predatory bacteria). However, it is noteworthy that apart from *Xanthobacter* with a relative abundance of 2.9% and a few species of *Bradyrhizobium* and *Pseudoxanthobacter*, there were numerous unidentified members belonging to the Xanthobacteraceae family, collectively accounting for over 13%. The *Azonexus* strain has been reported to possess both H_2 oxidation and N_2 fixation capabilities but lacks a CO_2 fixation pathway (Hu et al., 2022). *Methanobrevibacter arboriphilus* represents a prototypical hydrogenotrophic methanogenic archaea (Sharma et al., 2023), with certain strains exhibiting potential for N_2 fixation (Poehlein et al., 2018). *Hydrogenophaga* sp. NFH-34 harbors genes associated with N_2 fixation but is unable to perform this function for growth maintenance under hydrogen autotrophic conditions (Hu et al., 2022). Consequently, similar to *Stappia*, there is insufficient direct evidence supporting its N_2 fixation capability in the NF-HOB community. In general, besides the incompletely identified members of the Xanthobacteraceae family potentially involved in concurrent H_2 metabolism, CO_2 fixation, and N_2 fixation, other abundant species are likely to assume specific responsibilities and engage in symbiotic

cooperation.

The NF-HOB and ammonium-assimilation HOB communities exhibited significant abundance differences in 10 families and 28 genera. For NF-HOB, families with relatively higher relative abundance (averaging over 1%) included Spirosomaceae and Sphingomonadaceae (Fig. 5C), while the genera included *Xanthobacter*, *Pseudoxanthobacter*, and *Candidatus Kapaibacterium* (Fig. 5D). This observation can be attributed to the N_2 fixation capability of *Xanthobacter* and *Pseudoxanthobacter* (Arun et al., 2008).

The abundance of *Hydrogenophaga* showed a significant positive correlation ($p < 0.01$) with the abundance of various functional enzymes, including three hydrogenases (EC:1.12.1.2, EC:1.12.7.2, EC:1.12.99.6), carbonic anhydrase, glutamate dehydrogenase (EC:1.4.1.3), glutamate synthase, and glutamine synthase (Fig. 6A). This underscores the pivotal role played by this genus in processes such as H_2 oxidation and amino acid synthesis in NF-HOB communities. Among the other genera within the top 30 relative abundances, *Pseudopedobacter* and *Nubsella* displayed significant positive correlations ($p < 0.05$) with nitrogenase abundance. Additionally, *Nubsella* also demonstrated a strong correlation ($p < 0.01$) with hydrogenase (EC:1.12.1.2) abundance, as well as glutamate dehydrogenase (EC:1.4.1.3) and glutamate synthase. The abundance of *Muribaculum* showed a significantly positive association with Rubisco ($p < 0.05$), but the underlying mechanism is unknown.

The relative abundance of key functional enzymes in each HOB community is illustrated in Fig. 6B. The impact of nitrogen source supply conditions on these abundances was not decisive, which aligns with previous research findings (Wang et al.,

2024). Notably, the NF-HOB community enriched through continuous culture exhibited a remarkably high relative abundance of nitrogenase at 0.26%, surpassing that obtained through sequencing batch culture by at least 0.45 times. This phenomenon may be crucial for the community to adapt to the prescribed dilution rate and thrive, leading to the proliferation of distinct dominant genera. Moreover, even the abundance of nitrogenase obtained through sequencing batch culture offers significant advantages over previously investigated NF-HOB communities (HOB1) (Wang et al., 2024), as well as the N_2-fixing communities enriched in the microbial electrochemical system where water was electrolyzed for H_2 production (HOB2) (Zhang et al., 2022; Zhang et al., 2024) and the ammonium oxidation functional bacterial communities (AOB) (Fan et al., 2025) (Fig. 6C). Similarly, the relative abundance of the representative gene encoding nitrogenase, *nifH*, surpassed that of both previous NF-HOB communities (HOB1) and ammonium-assimilation HOB communities (HOB3, for its community structure, see supplementary material) (Fig. 6D). This substantial nitrogenase abundance ensures efficient autotrophic N_2 fixation to meet the demands for synthesizing MP.

3.4 Outlook

Selecting a high $R_{H/O}$ effectively enhanced the potential of NF-HOB, leading to remarkable achievements in MP synthesis during the later stage of sequencing batch culture, with a maximum titer reaching 983.26 mg/L, surpassing previous understanding. Other pivotal strategies implemented included ensuring a continuous supply of gas and optimizing the initial structure of the microbial community. Although the NF-HOB community exhibits a slightly lower proportion of MP and various

essential amino acids in CDW compared to the *Xanthobacter* pure strain, the latter necessitates a headspace gas composition of 78% N_2 and 2% O_2 (Hu et al., 2022; Sherbo et al., 2022), which may present challenges for large-scale pure cultivation. This study validates that air can effectively serve as a source of both nitrogen and oxygen for promoting biomass growth, thereby bringing NF-HOB closer to practical application.

Continuous culture outperforms sequencing batch culture in terms of MP volumetric productivity or biomass yield for the ammonium-assimilation HOB community (Matassa et al., 2016). However, in this study, an advantage in volumetric productivity was found only for the NF-HOB community. To further enhance this production level (2.297 mg/[L·h]), several considerations should be addressed in future work. Firstly, the adoption of large-scale equipment with improved gas-liquid mass transfer efficiency is necessary. Prolonging the duration of continuous cultivation can enhance community stability and facilitate the identification of more NF-HOB strains. Research on the CO_2 fixation performance of sulfur-oxidizing bacteria and nitrifying bacteria revealed that the extracellular free organic carbon (EFOC) inevitably produced exerted an inhibitory effect on the transcription of *cbb* genes, thereby impacting CO_2 sequestration (Zhang et al., 2021; Zhao et al., 2023). This feedback mechanism should also be taken into account in the cultivation of NF-HOB, particularly given the significant proportion of observed COD_s under continuous cultivation mode. Development techniques for isolating EFOC may therefore be deemed a pivotal strategy. Additionally, the exploration of optimal parameters can be enhanced by introducing supplementary gradients within the HRT range of 36 to 48 hours.

4. Conclusion

Under parallel operating conditions, a higher $R_{H/O}$ benefited NF-HOB biomass growth, resulting in a comparable final titer to that of ammonium-assimilation HOB. For the NF-HOB community, a N_2 fixation rate of 1.2-1.6 mg N_2 per gram dry biomass per hour was observed in the last two batches, resulting in the highest MP titer of 983 mg/L, with an amino acid composition similar to that of soybean meal. Continuous culture confirmed the specific growth rate of NF-HOB ranged from 0.021 to 0.028, leading to enhanced MP volumetric productivity. Substantial nitrogenase abundance ensured efficient autotrophic N_2 fixation to support MP synthesis.

Supplementary material

E-supplementary data for this work can be found in e-version of this paper online.

References

1. Allen, J. F., Thake, B., Martin, W. F., 2019. Nitrogenase inhibition limited oxygenation of earth's proterozoic atmosphere. Trends Plant Sci. 24 (11), 1022–1031.

2. Arun, A. B., Schumann, P., Chu, H. I., Tan, C. C., Chen, W. M., Lai, W. A., Kämpfer, P., Shen, F. T., Rekha, P. D., Hung, M. H., Chou, J. H., Young, C. C., 2008. *Pseudoxanthobacter* soli gen. nov., sp. nov., a nitrogen-fixing alphaproteobacterium isolated from soil. Int. J. Syst. Evol. Microbiol. 58 (7), 1571–1575.

3. Ehsani, E., Dumolin, C., Arends, J. B., Kerckhof, F. M., Hu, X., Vandamme, P., Boon, N., 2019. Enriched hydrogen-oxidizing microbiomes show a high diversity of co-existing hydrogen-oxidizing bacteria. Appl. Microbiol. Biotechnol. 103 (19), 8241–8253.

4. Fan, S., Song, Y., Zheng, D., Peng, X., Li, S., Gao, P., Li, D., 2025. Advancing autotrophic nitrogen removal in low C/N ratio wastewater: Innovative application of supercapacitor to enhance microbial electrolysis cells. J. Environ. Sci. 152, 87–98.

5. Greening, C., Kropp, A., Vincent, K., Grinter, R., 2023. Developing high-affinity, oxygen-insensitive [NiFe]-hydrogenases as biocatalysts for energy conversion. Biochem. Soc. Trans. 51 (5), 1921–1933.

6. Guo, L., Liu, S., Zhang, P., Hakeem, A., Song, H., Yu, M., Wang, F., 2024. Effects of different mulching practices on soil environment and fruit quality in peach orchards. Plants-Basel 13 (6), 827

7. Hu, X., Kerckhof, F. M., Ghesquière, J., Bernaerts, K., Boeckx, P., Clauwaert, P., Boon, N., 2020. Microbial protein out of thin air: fixation of nitrogen gas by an autotrophic hydrogen-oxidizing bacterial enrichment. Environ. Sci. Technol. 54 (6), 3609–3617.

8. Hu, X., Vandamme, P., Boon, N., 2022. Co-cultivation enhanced microbial protein production based on autotrophic nitrogen-fixing hydrogen-oxidizing bacteria. Chem. Eng. J. 429, 132535.

9. Ishizaki A, Tanaka K., 1990. Batch culture of *Alcaligenes eutrophus* ATCC 17697T using recycled gas closed-circuit culture system. J. Ferment. Bioeng. 69 (3), 170–174.

10. Kämpfer, P., Busse, H. J., Mclnroy, J. A., Xu, J., Glaeser, S. P. 2015, *Flavobacterium nitrogenifigens* sp. nov., isolated from switchgrass (*Panicum virgatum*). Int. J. Syst. Evol. Microbiol. 65 (Pt_9), 2803–2809.

11. Karr-Lilienthal, L. K., Grieshop, C. M., Spears, J. K., Fahey, G. C., 2005. Amino acid, carbohydrate, and fat composition of soybean meals prepared at 55 commercial

US soybean processing plants. J. Agric. Food Chem. 53 (6), 2146–2150.

12. Lu, S., Guan, X., Liu, C., 2020. Electricity-powered artificial root nodule. Nat. Commun. 11 (1), 1505.

13. Maheshwari, N., Kumar, M., Thakur, I. S., Srivastava, S., 2017. Recycling of carbon dioxide by free air CO_2 enriched (FACE) *Bacillus* sp. SS105 for enhanced production and optimization of biosurfactant. Bioresour. Technol. 242, 2–6.

14. Maimaiti, J., Zhang, Y., Yang, J., Cen, Y. P., Layzell, D. B., Peoples, M., Dong, Z., 2007. Isolation and characterization of hydrogen□oxidizing bacteria induced following exposure of soil to hydrogen gas and their impact on plant growth. Environ. Microbiol. 9 (2), 435–444.

15. Malik, K. A., Schlegel, H. G., 1981. Chemolithoautotrophic growth of bacteria able to grow under N_2-fixing conditions. FEMS Microbiol. Lett. 11 (1), 63–67.

16. Matassa, S., Boon, N., Verstraete, W., 2015. Resource recovery from used water: The manufacturing abilities of hydrogen-oxidizing bacteria. Water Res. 68, 467–478.

17. Matassa, S., Verstraete, W., Pikaar, I., Boon, N., 2016. Autotrophic nitrogen assimilation and carbon capture for microbial protein production by a novel enrichment of hydrogen-oxidizing bacteria. Water Res. 101, 137–146.

18. Poehlein, A., Schneider, D., Soh, M., Daniel, R., Seedorf, H., 2018. Comparative genomic analysis of members of the genera *Methanosphaera* and *Methanobrevibacter* reveals distinct clades with specific potential metabolic functions. Archaea 2018, 7609847.

19. Poudel, S., Pike, D. H., Raanan, H., Mancini, J. A., Nanda, V., Rickaby, R. E., Falkowski, P. G., 2020. Biophysical analysis of the structural evolution of substrate

specificity in RuBisCO. Proc. Natl. Acad. Sci. U. S. A. 117 (48), 30451–30457.

20. Scott, F., Yañez, L., Conejeros, R., Araya, B., Vergara-Fernández, A., 2021. Two internal bottlenecks cause the overflow metabolism leading to poly (3-hydroxybutyrate) production in *Azohydromonas lata* DSM1123. J. Environ. Chem. Eng. 9 (4), 105665.

21. Sharma, P., Parakh, S. K., Tsui, T. H., Bano, A., Singh, S. P., Singh, V. P., Lam, S. S., Nadda, A. K., Tong, Y. W., 2023. Synergetic anaerobic digestion of food waste for enhanced production of biogas and value-added products: strategies, challenges, and techno-economic analysis. Crit. Rev. Biotechnol. 1–21.

22. Sherbo, R. S., Silver, P. A., Nocera, D. G., 2022. Riboflavin synthesis from gaseous nitrogen and carbon dioxide by a hybrid inorganic-biological system. Proc. Natl. Acad. Sci. U. S. A. 119 (37), e2210538119.

23. Sorkhoh, N. A., Ali, N., Al-Awadhi, H., Dashti, N., Al-Mailem, D. M., Eliyas, M., Radwan, S. S., 2010. Phytoremediation of mercury in pristine and crude oil contaminated soils: Contributions of rhizobacteria and their host plants to mercury removal. Ecotox. Environ. Safe. 73 (8), 1998–2003.

24. Wang, H., Zhang, L., Tian, C., Fan, S., Zheng, D., Song, Y., Gao, P., Li, D., 2024. Effects of nitrogen supply on hydrogen-oxidizing bacterial enrichment to produce microbial protein: Comparing nitrogen fixation and ammonium assimilation. Bioresour. Technol. 394, 130199.

25. Weber, C. F., King, G. M., 2007. Physiological, ecological, and phylogenetic characterization of *Stappia*, a marine CO-oxidizing bacterial genus. Appl. Environ. Microbiol. 73 (4), 1266–1276.

26. Wiegel, J., Wilke, D., Baumgarten, J., Opitz, R., Schlegel, H. G., 1978. Transfer of

the nitrogen-fixing hydrogen bacterium Corynebacterium autotrophicum Baumgarten et al. to *Xanthobacter* gen. nov. Int. J. Syst. Bacteriol. 28 (4), 573–581.

27. Woern, C., Grossmann, L., 2023. Microbial gas fermentation technology for sustainable food protein production. Biotechnol. Adv. 69, 108240.

28. Yu, J., Lu, Y., 2019. Carbon dioxide fixation by a hydrogen-oxidizing bacterium: biomass yield, reversal respiratory quotient, stoichiometric equations and bioenergetics. Biochem. Eng. J. 152, 107369.

29. Zacarias, S., Temporão, A., Barrio, M. D., Fourmond, V., Léger, C., Matias, P. M., Pereira, I. A., 2019. A hydrophilic channel is involved in oxidative inactivation of a [NiFeSe] hydrogenase. ACS Catal. 9 (9), 8509–8519.

30. Zhang, L., Tian, C., Wang, H., Gu, W., Zheng, D., Cui, M., Wang, X., He, X., Zhan, G., Li, D., 2022. Improving electroautotrophic ammonium production from nitrogen gas by simultaneous carbon dioxide fixation in a dual-chamber microbial electrolysis cell. Bioelectrochemistry 144, 108044.

31. Zhang, S., Wang, L., Fu, X., Tsang, Y. F., Maiti, K., 2021. A continuous flow membrane bio-reactor releases the feedback inhibition of self-generated free organic carbon on *cbb* gene transcription of a typical chemoautotrophic bacterium to improve its CO_2 fixation efficiency. Sci. Total Environ. 761, 143186.

32. Zhang, L., Wang, J., Fu, G., Zhang, Z., 2020a. Simultaneous electricity generation and nitrogen and carbon removal in single-chamber microbial fuel cell for high-salinity wastewater treatment. J. Clean Prod. 276, 123203.

33. Zhang, L. J., Xie, Y., Ding, L. Y., Qiao, X. J., Tao, H. C., 2020b. Highly efficient ammonium removal through nitrogen assimilation by a hydrogen-oxidizing bacterium,

Ideonella sp. TH17. Environ. Res. 191, 110059.

34. Zhang, L., Zeng, L., Wang, J., Wang, H., Zheng, D., Wang, X., Li, D., Zhan, G., 2024. Enhanced microbial protein production from CO_2 and air by a MoS2 catalyzed bioelectrochemical system. ChemPlusChem e202400072.

35. Zhao, X., Zhang, Y., Chen, L., Zhang, S., Fu, X., Wang, L., 2023. Continuous-flow membrane bioreactor enhances enrichment and culture of autotrophic nitrifying bacteria by removing extracellular free organic carbon. Environ. Sci. Pollut. Res. 30 (14), 42378–42389.

Figure captions:

Fig. 1 Characterization of biomass growth, pH change, and N element flow during sequencing batch culture of HOB communities (NF: NF-HOB community; NA: ammonium-assimilation HOB community) at $R_{H/O}$ = 3.5: (A) COD_t concentration, pH change, and CDW concentration; (B) NH_4^+-N (AN) and TN_s concentrations; (C) carbon and nitrogen content and C/N ratio in biomass (*C. necator* as reference); (D) changes in TN_s and $TN_{biomass}$.

Fig. 2 Characterization of biomass growth, pH change, and soluble-nitrogen variation during sequencing batch culture of HOB communities (NF: NF-HOB community; NA: ammonium-assimilation HOB community) at $R_{H/O}$ = 7: COD_t concentration, pH change, and CDW concentration in the first (A), second (B) and third (C) batches; NH_4^+-N (AN) and TN_s concentrations in the first (D) and second (E) batches.

Fig. 3 (A) Carbon and nitrogen content and C/N ratio in biomass of HOB communities at $R_{H/O}$ = 7 and (B) changes in TN_s and $TN_{biomass}$ during each sequencing batch; NF1,

NF2, and NF3 represent the NF-HOB community in the first, second, and third batches, respectively; NA1 and NA2 represent the ammonium-assimilation HOB community in the first and second batches, respectively. (C) Amino acids profile of high-titer biomass (this study), compared with soybean meal reported and the NF-HOB community previously enriched within small-scale systems (His: Histidine; Ile: Isoleucine; Leu: Leucine; Lys: Lysine; Met: Methionine; Phe: Phenylalanine; Thr: Threonine; Val: Valine; Arg: Arginine; Asp: Aspartate; Glu: Glutamate; Ser: Serine; Gly: Glycine; Ala: Alanine; Tyr: Tyrosine; Pro: Proline).

Fig. 4 (A) COD_t concentration during continuous culture of the NF-HOB community at HRT = 24 h; COD_t (inner): COD_t of the liquid-phase reaction system; COD_t (outlet): daily average COD_t of liquid pumped out of the system. (B) Inner COD_t concentration, COD_s concentration, pH, and the ratio of COD_s to COD_t ($Ratio_{CODs}$) during continuous culture of the NF-HOB community at HRT = 48 h. (C) Biomass yield of the NF-HOB community enriched during the third batch culture (NF3) and continuous culture (NFC) (Each value is the mean ± standard deviation of triplicates, “NS” indicates no significant difference because the two-tailed p-value of the t-test is > 0.05).

Fig. 5 Microbial community structure and difference analysis: species distribution at the family (A) and genus (B) levels (IBC: HOB community used for sequencing batch culture experiments after initial domestication; N1: NF-HOB community enriched at $R_{H/O}$ = 3.5; N2: NF-HOB community enriched during the first batch at $R_{H/O}$ = 7; N3: NF-HOB community enriched during the second batch at $R_{H/O}$ = 7; N4: NF-HOB community enriched during the third batch at $R_{H/O}$ = 7; NH1: ammonium-assimilation HOB community enriched at $R_{H/O}$ = 3.5; NH2: ammonium-assimilation HOB community enriched during the first batch at $R_{H/O}$ = 7; NH3: ammonium-assimilation HOB community enriched during the second batch at $R_{H/O}$ = 7; NC: NF-HOB community enriched during the continuous culture); volcano plot of species with significant abundance differences between NF-HOB and ammonium-assimilation HOB communities at the family (C) and genus (D) level ("Up" indicates that the abundance of the species represented by this point is significantly higher in the NF-HOB

community, while "Down" indicates the opposite).

Fig. 6 (A) Heatmap of Spearman correlation coefficients between the abundance of key functional enzymes and the abundance of dominant genera (* indicates the two-tailed p-value of the t-test is < 0.05, ** indicates the two-tailed p-value of the t-test is < 0.01). (B) Relative abundance of functional enzymes. (C) Comparison of the relative abundance of nitrogenase in microbial communities (HOB_SBR: HOB communities enriched during sequencing batch culture in this study; HOB1: previously reported NF-HOB communities; HOB2: previously reported N_2-fixing bacterial communities enriched in H_2-producing electrolytic cells; AOB: previously reported ammonium-oxidizing functional bacterial communities). (D) Comparison of the relative abundance of *nifH* in microbial communities (HOB3: ammonium-assimilation HOB communities). (In the violin plot, the purple dots indicate the mean value, and the length of the whisker lines represents the size of the standard deviation.)

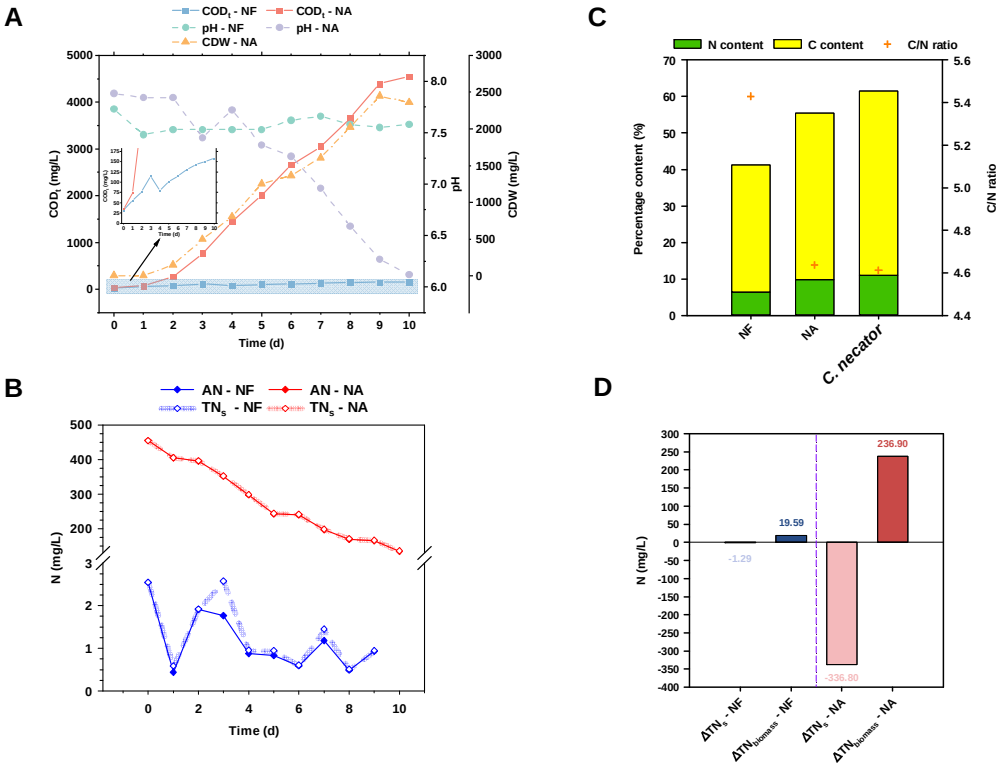
A
COD$_t$ - NF
COD$_t$ - NA
pH - NF
pH - NA
CDW - NA
COD$_t$ (mg/L)
pH
CDW (mg/L)
Time (d)
B
AN - NF
AN - NA
TN$_s$ - NF
TN$_s$ - NA
N (mg/L)
Time (d)
C
N content
C content
C/N ratio
Percentage content (%)
C/N ratio
NF
NA
C. necator
D
N (mg/L)
19.59
-1.29
236.90
-336.80
ΔTN$_s$ - NF
ΔTN$_{biomass}$ - NF
ΔTN$_s$ - NA
ΔTN$_{biomass}$ - NA

Fig. 1

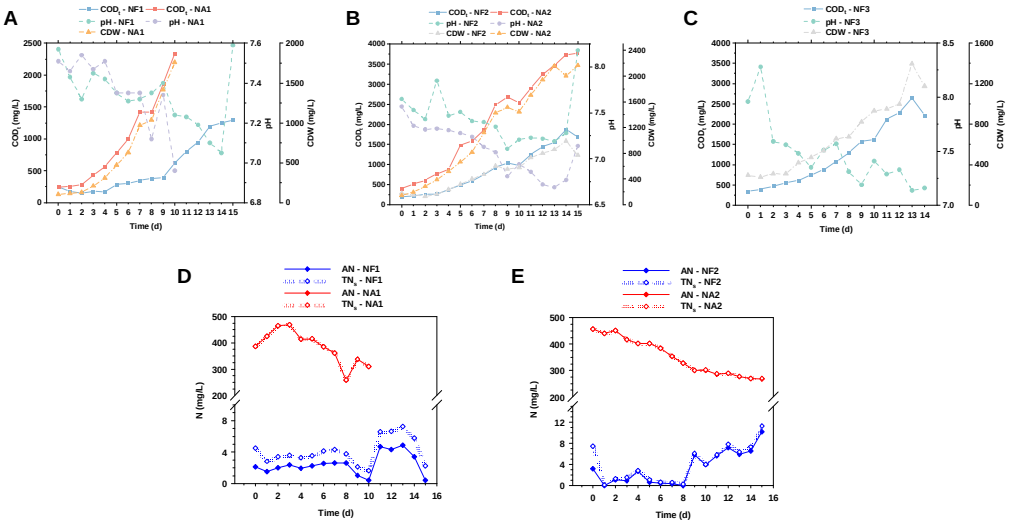
A
COD$_t$ - NF1
COD$_t$ - NA1
pH - NF1
pH - NA1
CDW - NA1
COD$_t$ (mg/L)
pH
CDW (mg/L)
Time (d)
B
COD$_t$ - NF2
COD$_t$ - NA2
pH - NF2
pH - NA2
CDW - NF2
CDW - NA2
COD$_t$ (mg/L)
pH
CDW (mg/L)
Time (d)
C
COD$_t$ - NF3
pH - NF3
CDW - NF3
COD$_t$ (mg/L)
pH
CDW (mg/L)
Time (d)
D
AN - NF1
TN$_t$ - NF1
AN - NA1
TN$_t$ - NA1
N (mg/L)
Time (d)
E
AN - NF2
TN$_t$ - NF2
AN - NA2
TN$_t$ - NA2
N (mg/L)
Time (d)

Fig. 2

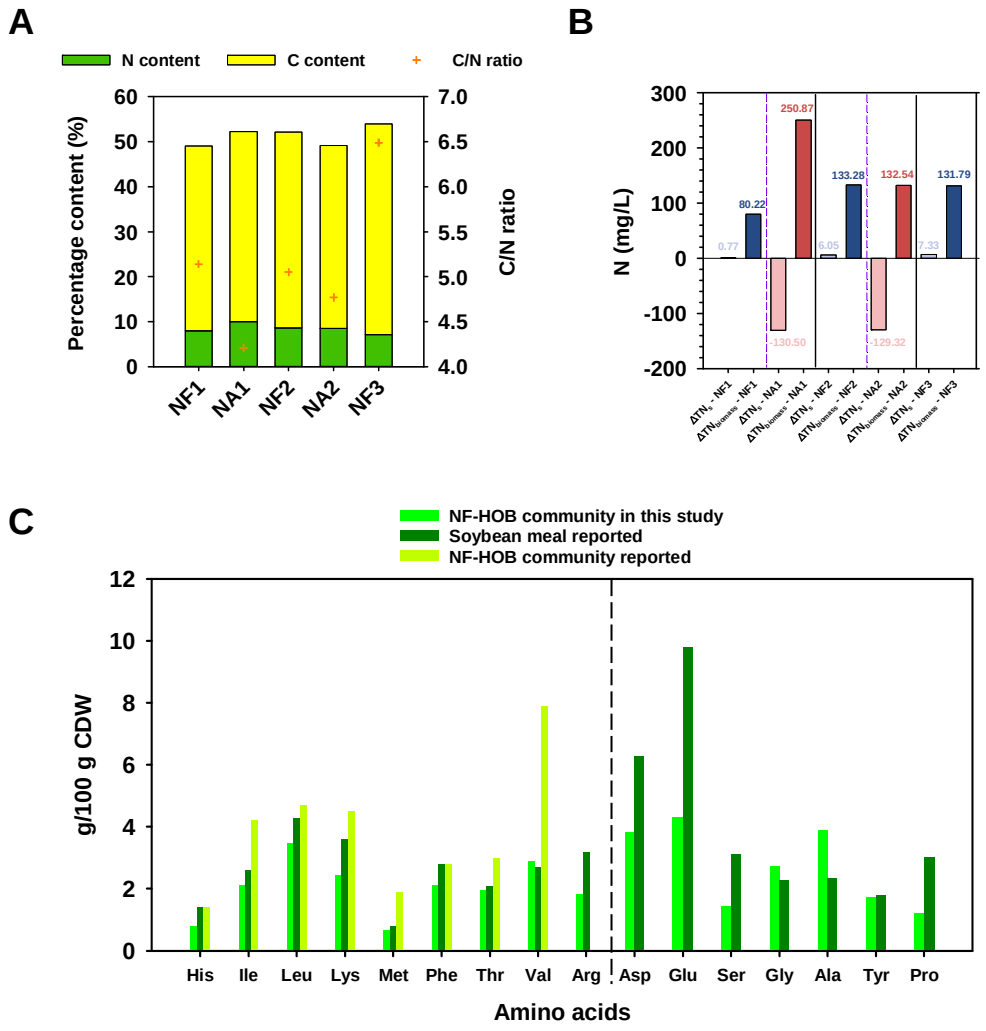
A
N content
C content
C/N ratio
Percentage content (%)
C/N ratio
NF1
NA1
NF2
NA2
NF3
B
N (mg/L)
250.87
80.22
133.28
132.54
131.79
0.77
6.05
7.33
-130.50
-129.32
C
NF-HOB community in this study
Soybean meal reported
NF-HOB community reported
g/100 g CDW
His
Ile
Leu
Lys
Met
Phe
Thr
Val
Arg
Asp
Glu
Ser
Gly
Ala
Tyr
Pro
Amino acids

Fig. 3

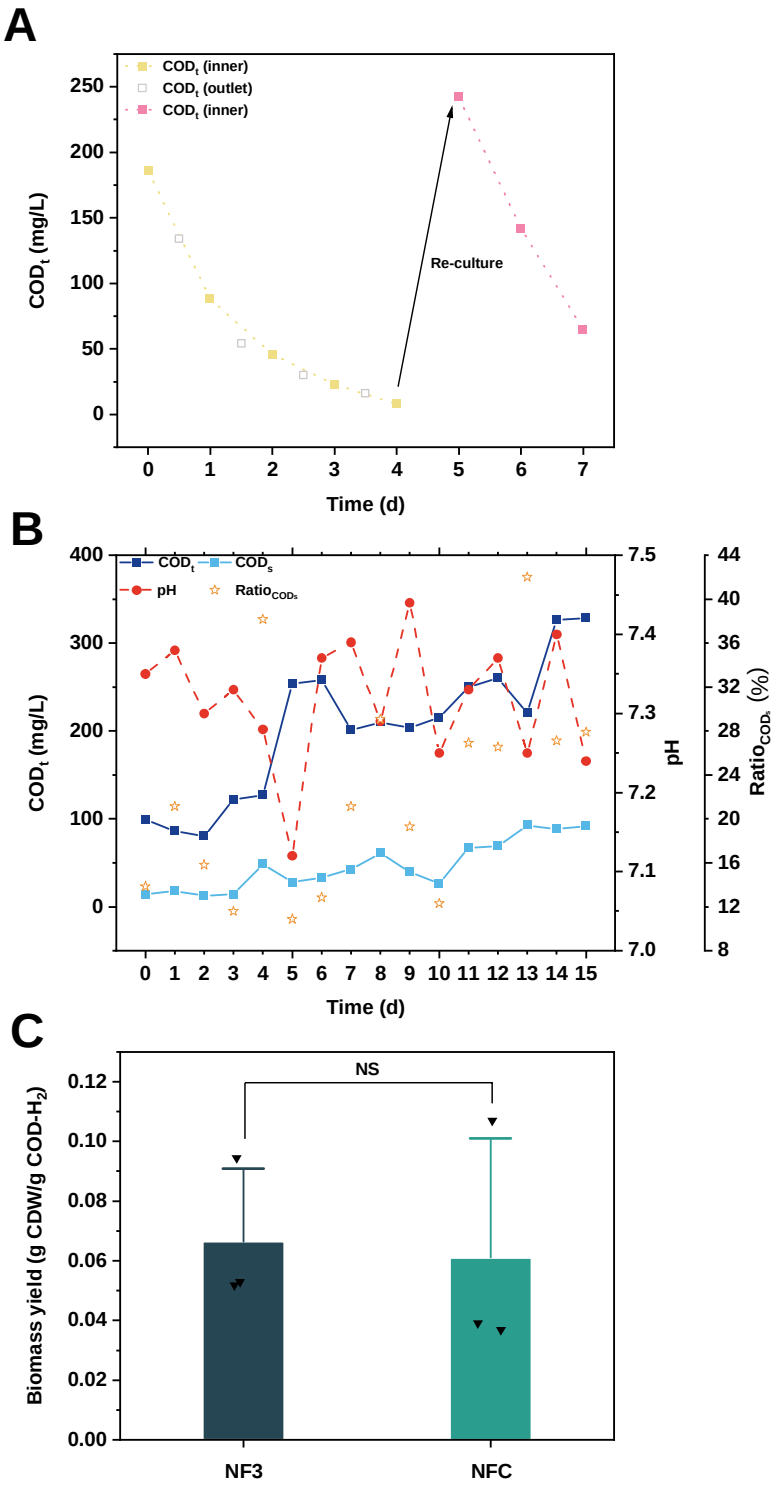
A
COD$_t$ (inner)
COD$_t$ (outlet)
COD$_t$ (inner)
Re-culture
COD$_t$ (mg/L)
Time (d)
B
COD$_t$
COD$_s$
pH
Ratio$_{COD_s}$
COD$_t$ (mg/L)
pH
Ratio$_{COD_s}$ (%)
Time (d)
C
NS
Biomass yield (g CDW/g COD-H$_2$)
NF3
NFC

Fig. 4

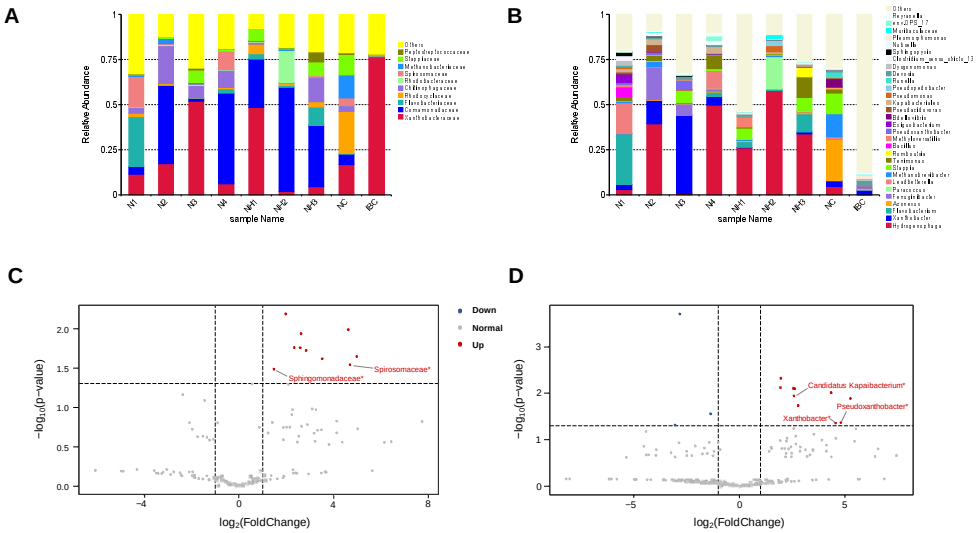
A
B
C
D
Relative Abundance
sample Name
N1
N2
N3
N4
NH1
NH2
NH3
NC
BC
Down
Normal
Up
Spirosomaceae*
Sphingomonadaceae*
Candidatus Kapaibacterium*
Pseudoxanthobacter*
Xanthobacter*
−log10(p−value)
log2(FoldChange)

Fig. 5

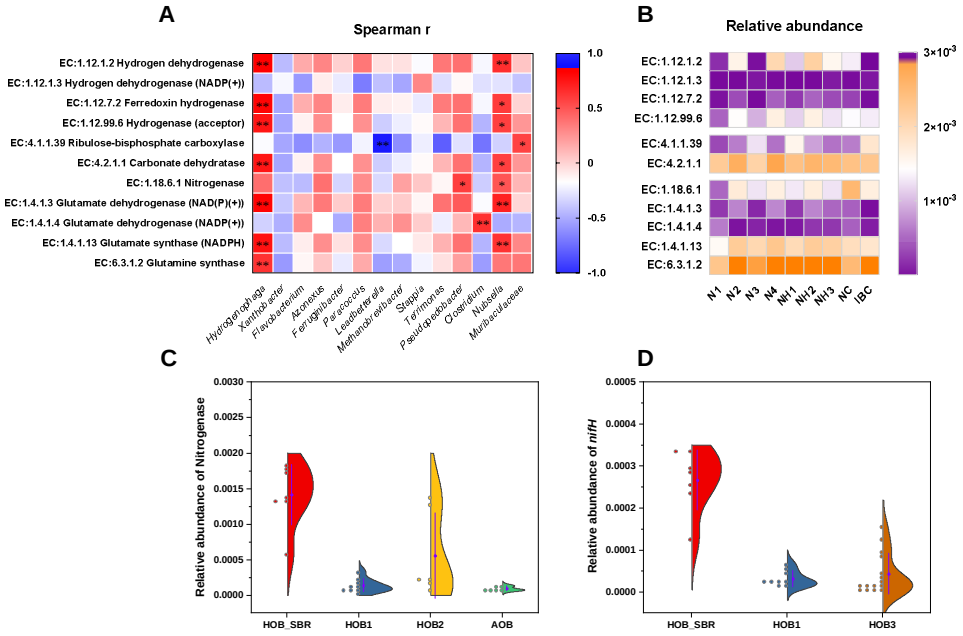
A
Spearman r
EC:1.12.1.2 Hydrogen dehydrogenase
EC:1.12.1.3 Hydrogen dehydrogenase (NADP(+))
EC:1.12.7.2 Ferredoxin hydrogenase
EC:1.12.99.6 Hydrogenase (acceptor)
EC:4.1.1.39 Ribulose-bisphosphate carboxylase
EC:4.2.1.1 Carbonate dehydratase
EC:1.18.6.1 Nitrogenase
EC:1.4.1.3 Glutamate dehydrogenase (NAD(P)(+))
EC:1.4.1.4 Glutamate dehydrogenase (NADP(+))
EC:1.4.1.13 Glutamate synthase (NADPH)
EC:6.3.1.2 Glutamine synthase
Hydrogenophaga
Xanthobacter
Flavobacterium
Azonexus
Ferrugibacter
Paracoccus
Leadbetterella
Methanobrevibacter
Steppia
Terrimonas
Pseudopedobacter
Clostridium
Nubsella
Muribaculaceae
1.0
0.5
0
-0.5
-1.0
B
Relative abundance
EC:1.12.1.2
EC:1.12.1.3
EC:1.12.7.2
EC:1.12.99.6
EC:4.1.1.39
EC:4.2.1.1
EC:1.18.6.1
EC:1.4.1.3
EC:1.4.1.4
EC:1.4.1.13
EC:6.3.1.2
N1
N2
N3
N4
NH1
NH2
NH3
NC
IBC
3×10-3
2×10-3
1×10-3
C
Relative abundance of Nitrogenase
0.0030
0.0025
0.0020
0.0015
0.0010
0.0005
0.0000
HOB_SBR
HOB1
HOB2
AOB
D
Relative abundance of nifH
0.0005
0.0004
0.0003
0.0002
0.0001
0.0000
HOB_SBR
HOB1
HOB3

Fig. 6

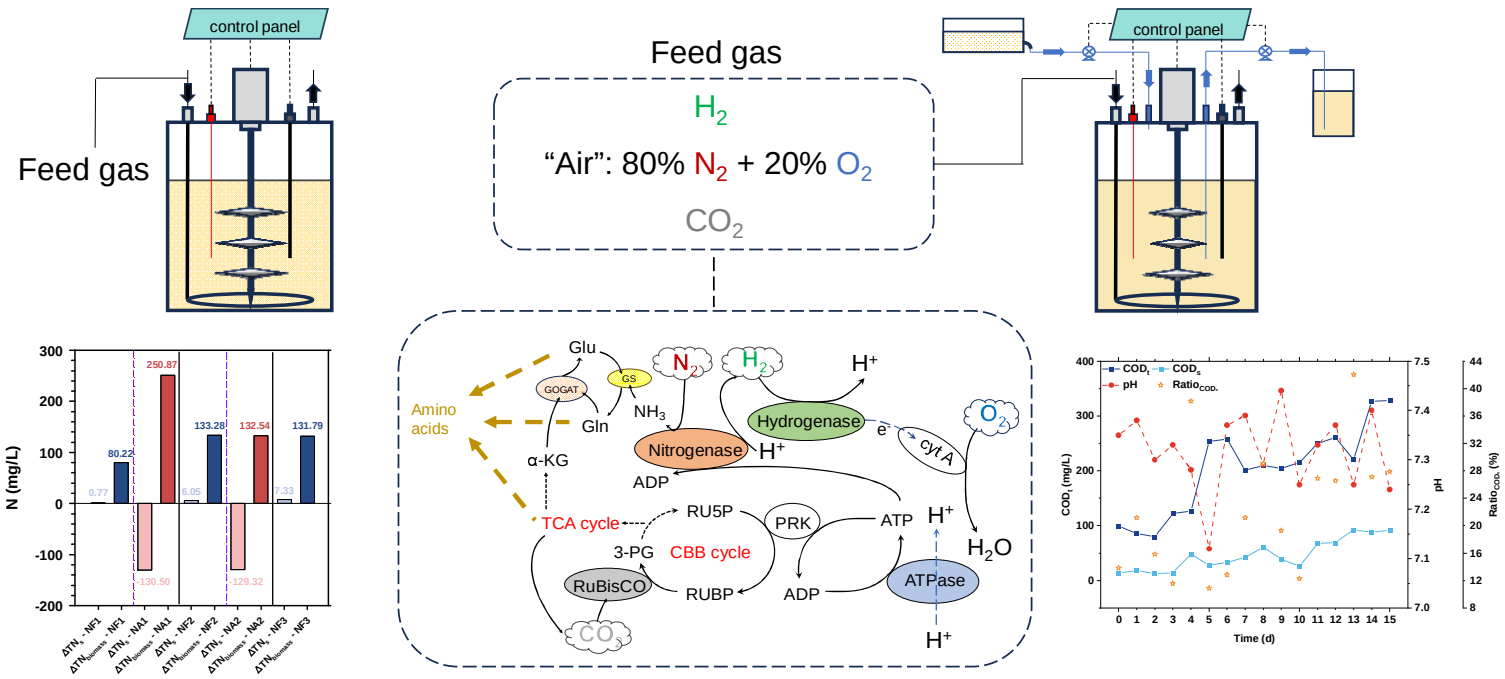

H_2 to O_2 ratio = 7

Nitrogen-fixing hydrogen-oxidizing bacterial community

HRT = 48 h

N_2 fixation rate:
1.2-1.6 mg N_2 / g CDW / h
MP titer:
983 mg/L

MP volumetric productivity:
2.297 mg/(L·h) ↑
Biomass yield:
0.11 g CDW / g COD-H_2

Microbial protein